LIMNOLOGY
and
OCEANOGRAPHY: METHODS

Limnol. Oceanogr.: Methods 8, 2010, 403–413

Correcting porewater concentration measurements from peepers: Application of a reverse tracer

Burt Thomas and Michael A. Arthur*
Department of Geosciences, Penn State University, University Park, PA

Abstract

This work describes the routine application of a reverse tracer to passive diffusion sampler deployments. The reverse tracer provides evidence of the extent of equilibrium for any peeper cell and an indication of the diffusivity change with depth associated with physical changes in the sediment. Quantitative measurement of the reverse tracer also allows for the correction of measured data within cells that may not have reached chemical equilibrium, thereby removing the requirement of a priori knowledge of the time to concentration equilibrium. Investigations that use ion chromatographic techniques that incidentally measure Br^- or other conservative tracers can apply this method with no additional analytical requirements. Our approach opens up peeper applications to shorter duration deployments as required for marine sediment sampled by submersibles and deployments in environments with uncertain or unknown equilibration times such as highly heterogeneous sediments. We present a novel peeper design as well as the theory and application of this technique along with an example from a field deployment. We conclude that corrections that assume a simple approximation of exponential tracer decay are a considerable improvement over the reliance on observed measured values from porewater dialysis samplers. Moreover, even without using the reverse tracer to correct measured cell concentrations, the reverse tracer can point to significant divergences from concentration equilibrium and is useful to determine which cell measurements should be discarded.

Obtaining representative water samples from difficult sample matrices is a common bugaboo of wetland biogeochemists. Wetland soils and shallow marine sediments exhibit remarkable spatial heterogeneity in chemical (Lewandowski et al. 2002), biological (Brandl et al. 1993), and physical properties, including porosity (Blodau and Moore 2002). Filtration, centrifugation (Lyons et al. 1979), suction sampling, and core-squeezing (Bender et al. 1987; Reeburgh 1967) are destructive sampling techniques that complicate simultaneous sampling of dissolved ions and gases. Furthermore, many sediment types such as woody peats or rocky sediments are difficult or impossible to core. One popular sampling approach that can be both passive and in situ is the deployment of passive diffusion cells with which porewaters equilibrate (Hesslein 1976; Mayer 1976; Sayles et al. 1973).

These passive diffusion samplers, commonly termed peepers, are popular tools in wetland and sediment biogeochemistry because they result in size-filtered samples and can be easily deployed and sampled at modest cost and effort in sediments and soils (LaForce et al. 1999). Nearly all peeper designs in the literature consist of a series of isolated volumes of water surrounded by a membrane on one or more sides. These membranes allow for solute diffusion in and out but exclude the entry of particles, organisms, and sediment matrix materials. The peeper cell internal concentrations are effectively homogeneous on the order of a few hours owing to high diffusivities in water, and the volume of the peeper cell relative to the formation pore volume with which it equilibrates is assumed to be negligible. Further, most peeper studies use an isotonic internal solution that minimizes osmotic effects due to water activity differences on either side of the membrane. The use of peepers is therefore usually restricted to the measurement of minor components in water. Unfortunately, peeper users face a difficult conundrum: how can one know the time it takes for a peeper cell to reach concentration equilibrium with the surrounding sediment if the properties of the surrounding sediment are unknown?

This work describes a novel peeper design and a routine application of a reverse tracer to peeper cells that allows inves-

*Corresponding author: E-mail: burt_thomas@usgs.gov

Acknowledgments

This work was supported by a grant from the American Chemical Society (ACS) Petroleum Research Fund, PRF-44729-AC2, to M. A. Arthur and B. Thomas, and by initial seed funding to B. Thomas from the Penn State Biogeochemical Research Initiative for Education (BRIE) sponsored by National Science Foundation Integrative Graduate Education and Research Traineeship (NSF-IGERT) grant DGE-9972759.

DOI 10.4319/lom.2010.8.403

tigators to characterize the outward diffusion of a tracer and apply a cell-specific correction for the concentration of each inward-diffusing solute. We demonstrate the reverse tracer approach through field application and laboratory demonstration of the concept, and finally use a mathematical simulation to justify the form of the equation used for the correction.

This is a simple qualitative method to estimate both the depth- and location-dependent changes in peeper cell equilibration times, and it can be a quantitative method to correct measured cell concentrations for these differences. This new technique allows for a single peeper deployment to obtain reliable concentration measurements for each cell in heterogeneous sediments, alleviating the need for complete and unknown equilibration times that result in very long peeper deployments in consolidated sediment. Our approach opens up peeper applications to shorter-duration deployments with submersibles (Dattagupta et al. 2007) and deployments in environments with uncertain or unknown equilibration times.

Materials and procedures

Peeper construction—Terrestrial bogs replete with woody debris and complex peat matrices present a particular challenge to alternative methods of porewater sampling. To demonstrate the use of this technique in nature, we describe a peeper intended for repeated deployment into a permanently installed PVC casing. Such peepers have been in use for 4 years to obtain long-term measurements of bog porewater constituents, including gas and anion samples.

Peepers are constructed from 2-inch PVC pipes and a solid PVC rod that was machined to slide easily inside the PVC pipe. The pipe is perforated and is used as a permanently installed casing that facilitates resampling and replacement to the exact location and orientation within the sediment profile. Segments of similar PVC rod are machined to make small cones that fit snugly into the end of the perforated pipe and cemented or nailed into place. Small, cylindrical, flat-bottom holes are drilled perpendicularly into the PVC rod (parallel to the radius) and are separated by 5 cm along the length of the rod and offset 120 degrees from each other. The result is an evenly spaced spiral arrangement of small cylindrical holes in a long PVC rod. The holes are designed to accommodate small 5-cc peeper cells. These peeper cells are constructed from 5-cc Nalgene cups, with 0.2-μm, 45-mm polypropylene filters (Pall Life Sciences) attached like a drum skin by means of small 4-mm silicone dental elastics obtained from a local orthodontist (GAC Inc.). These peeper cell cups and membranes are inexpensive, chemically inert, and hydrophilic. Further, they have a relatively large area/volume ratio, as the aspect ratio between the length, height, and width is approximately 1:1:1. A diagram of the peeper is shown in Fig. 1. One important addition to the design is a diagonal, downward-sloping drill hole at the back of the cell cavity in the central rod. This hole is necessary for air trapped around the back of the peeper cell to escape upward while the peeper is slowly deployed into its submerged casing and minimizes the entrainment of air during deployment. The initial installation of a peeper casing will likely change the surrounding sediment characteristics; however, since this occurs only once upon initiation of the measurements, it is not rele-

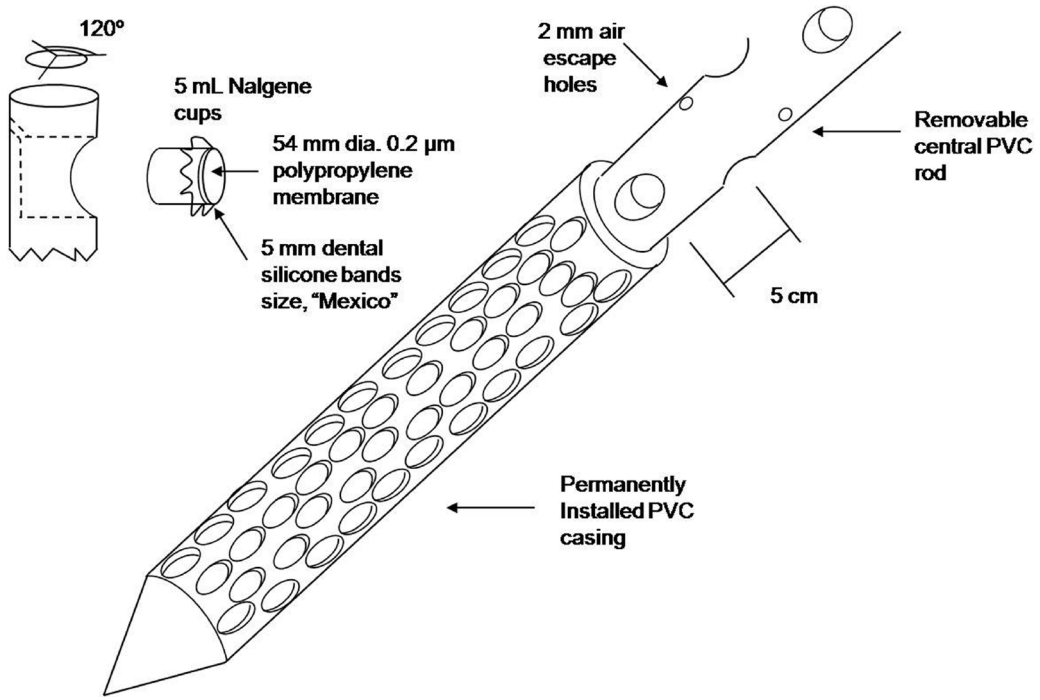

Fig. 1. Peeper casing and rod design. All materials are readily available at hardware stores or scientific catalogs. The total cost of the device is less than $40 per peeper, excluding labor costs.

vant for time-series studies. In addition, the tight-fitting rod and casing design minimize the likelihood of the peeper rod acting as a preferential flow path. This design has not been tested for an artesian flow regime where a positive pressure gradient could drive flow upward along the casing.

Peeper cells are first prepared in a large tub of distilled, deionized water (DDI) and known tracer content. In our case, we added a concentrated solution of KBr to the large tub, equivalent to a final KBr tracer concentration of 200 μM. The cells are constructed from filters and elastics underwater by hand to ensure that no air bubbles are present in the cells, and the elastics are seated securely underneath the lip of the Nalgene cups. Once all cells are created, they are placed, along with the remaining tracer solution, in a large, airtight, 50-L drum-style sports water cooler equipped with a screw lid with plastic underside gasket. The lid is fitted with two bulkhead Swagelock fittings and connected to an N_2 gas purge line with submerged air stone. The peeper cells are left to be purged and equilibrate with the tracer solution for approximately 3 days under a constant N_2 purge gas stream flowing at ~100 mL/min. After 3 days, the sports cooler is pressurized with N_2 and sealed for transport to the field. Once in the field, the peeper cells are loaded into the rod (approximately 10–15 cells per rod depending on the desired sampling depths) within minutes of opening the container, and the rod is inserted into the previously installed peeper casing.

Porewater sampling and analysis—To sample gas and anion constituents, the rod is removed from the casing and each peeper cell is removed one at a time and placed on a flat surface. The surface of the cell can be rinsed with a distilled water squirt bottle briefly, and a gas-tight syringe with needle is used to extract 2 mL water for dissolved gas analysis. The solution in the gas-tight syringe is injected into a preflushed acidified serum vial for headspace gas analysis. The now-pierced membrane can be removed, and a standardized and calibrated pH/ORP (oxidation reduction potential) probe is placed into the Nalgene container for analysis of reduction potential and pH. The remaining solution after this measurement is stored on ice in cryovials for anion analyses (Br^-, Cl^-, acetate, sulfate, phosphate) via ion chromatography (Dionex DX2000). Sampling requires approximately 45 s to remove, rinse, and sample each cell, resulting in a sampling time of approximately 10 min.

Care must be taken to sample the most oxygen-sensitive constituents first. Once the wetted membrane is pierced, air diffuses into the cells rapidly. The deepest cells are usually furthest from equilibrium, so we recommend sampling from the bottom cell upward and waiting to measure pH until all porewater gas subsamples have been removed. This is especially true in very cold porewaters, since the pH probe response time can be longer.

The data from a 7-day deployment to Bear Meadows Natural Area, Centre County, Pennsylvania, in December 2004 are presented in Fig. 2. The starting cell bromide concentration was 200 μM, and the background formation Br concentration was less than 1 μM at all depths. The increasing concentration of bromide remaining in the cell with depth is shown in Fig. 2a along with the change in ORP values associated with a transition from the fibrous acrotelm to denser peat catotelm matrix. In general, the high porosity (>90%) and fibrous nature of acrotelm (surface) peat results in sediment diffusivities that are very near those in water, so there is little need for a peeper correction in shallow peeper cells given at least 1 day to equilibrate. Cells below this transition, however, are significantly impacted by lower sediment diffusivities, and with depth, the need for a correction increases. The sediment mineral content is very low throughout the cores (1% to 5% by weight), so diffusivity differences with depth are likely due simply to peat density. We have also compared the measured cell ion concentrations to the values that result from three separate treatments of the correction described in the subsequent sections in Fig. 2b–e.

Theoretical approach to correcting measured values—Fick's first law for one-dimensional transport across a membrane describes the proportional dependence of solute flux through a membrane, J (mol/m^2/s), on the concentration gradient across the membrane, $\_C$ (mmol/m^3). For a given membrane, which has a constant outside concentration and permeation speed, k_m (m/s), the mass flux law can be written as

$$J = k_m \_C. \tag{1}$$

For a given solute and peeper cell of constant volume, V (m^3), and membrane area, A (m^2), the time rate of change of mass across the membrane with the above mass flux condition is equivalent to

$$\frac{d}{dt} C_{peeper} = -k_m * \frac{A}{V} * (C_{peeper} - C_{outside}). \tag{2}$$

For invariant A, V, k_m, formation concentration ($C_{outside}$), and an initial cell concentration of zero (peeper cell concentration, C_{peeper}), this can be integrated to describe the inward diffusion of a species:

$$C_p(t) = C_{outside}(1 - e^{-\frac{k_m tA}{V}}). \tag{3}$$

This expression describes the time-dependent concentration within the cell for situations in which membrane permeation is slow relative to diffusion of ions from the formation to the outside membrane surface. The constants related to the solute–membrane interaction can be lumped into a single constant

$$-k_m * \frac{A}{V},$$

that is unique for any solute in a given peeper cell at a particular temperature. More generally, we can describe both the outward and inward diffusion of a species by the following expression:

$$\Delta C_p = \Delta C_i(1 - e^{-Kt}), \tag{4}$$

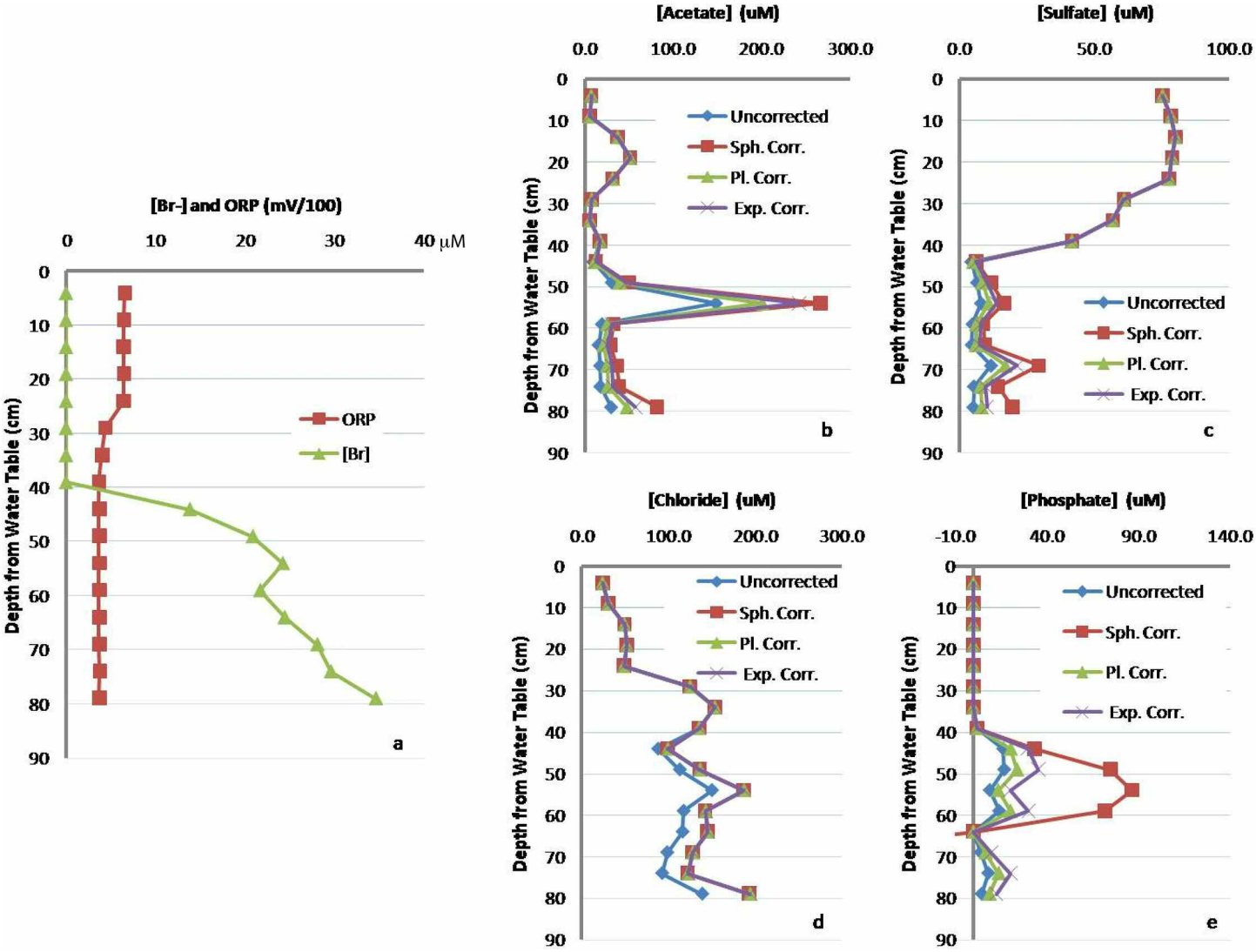

Fig. 2. Porewater data from a 1-week peeper deployment, including measured cell values for selected ions and values resulting from corrections based on the spherical, planar, and exponential decay curves described in the text.

in which $\Delta C_p = C^t_p - C^i_p$ and $\Delta C_i = C^i_{out} - C^i_p$. The concentration of tracer inside the peeper is C^i_p, and the concentration inside the peeper at any time is C^t_p. If $\Delta C_i > 0$, species diffuse inward, and if $\Delta C_i < 1$ species diffuse outward.

The use of a conservative reverse tracer requires the addition of a known concentration of chemically unreactive salt, KBr in our case, to a solution used to fill the peeper cells. If the concentration of tracer in the formation is negligible, the above analytical expression can be simplified to a form consistent with exponential decay of an internal tracer concentration:

$$-\frac{1}{t}\ln(C^t_p / C^i_p) = K_{Br}. \qquad (5)\text{Q1}$$

Because the initial concentration of tracer inside the peeper, C^i_p, and the length of deployment are known, and we measure the final concentration inside the peeper, C^t_p, we know three of the four variables in Eq. (5) and solve for the constant K_{Br}, which empirically blends sediment characteristics into a single estimate of the effective diffusivity. Following an assumption by Webster et al. (1998), we also assume that for a given membrane or sediment, the permeability of two species are related by the ratio of their free diffusion constants. It follows that we can calculate a new K_i for any species with knowledge of the empirically derived K_{Br}, using the following expression:

$$K_i = \frac{D_i}{D_{Br}} K_{Br}. \qquad (6)$$

Values of D_i, the diffusivity of an ion in dilute aqueous solution, are readily available in the literature (Hayduk and Laudie 1974; Li and Gregory 1974). We have compiled a few common D_i values in Table 1.

Table 1. Select tabulated values of the tracer diffusion coefficients and the calculated ratio, D_i/D_{Br}.

Ionic Solute	D_i (× 10^{-6}) 25°C	D_i/D_{Br}	Neutral Solute	D_i (× 10^{-6}) 25°C	D_i/D_{Br}
Cl^-	20.3	1.01	H_2	44	2.19
F^-	14.6	0.73	He	62.8	3.12
OH^-	52.7	2.62	N_2	19.9	0.99
Br^-	20.1	1.00	O_2	22.9	1.14
SO_4^{2-}	10.7	0.53	CO_2	19.2	0.96
NO_3^-	19	0.95	H_2S	21	1.04
CO_3^{2-}	9.55	0.48	CH_4	16.7	0.83
HPO_4^{2-}	7.34	0.37	C_2H_6	13.8	0.69
NH_4^+	19.8	0.99	NH_3	22.8	1.13
K^+	19.6	0.98	Ar	19.8	0.99
Na^+	13.3	0.66	Urea	13.8	0.69
H^+	93.1	4.63	Ethanol	12.4	0.62
Mg^{2+}	7.05	0.35	Sucrose	5.2	0.26
Mn^{2+}	6.88	0.34	Acetic acid	11.9	0.59
Ca^{2+}	7.93	0.39	Butyric acid	9.2	0.46
Fe^{2+}	7.19	0.36			
Al^{3+}	5.59	0.28			

Values are from Li and Gregory (1974) and Hayduk and Laudie (1974).

Using the calculated K_i values for a given solute, we can now solve equation (4) for the external concentration of an inward-diffusing solute by assuming that the initial concentration of solute in the peeper cell is zero, $C_p^i = 0$. Equation (4) rearranges and becomes

$$C_{out}^i = C_p^t / (1 - e^{-K_i t}) . \quad (7)$$

This simple equation can be used to correct measured porewater values given a measurement of the remaining tracer concentration in any cell.

Assessment

We used three different approaches to demonstrate the theory of this reverse tracer. We performed a simple bench-top experiment to demonstrate the concept in the laboratory, created a mathematical model to simulate the system in sediments, and applied the correction to a set of peeper samples collected as described above.

For our bench-top experiment, we obtained a time-series of peeper cell concentrations to demonstrate the ability to use the tracer concentration to correct for the concentration disequilibrium. For this experiment, 6 beakers of 1-L volume were filled with a solution of 125 µM KCl. Peeper cells of 5-mL volume were assembled with an internal concentration of 100 µM KBr and 25 µM KCl. All chemicals are reagent grade (Fisher Scientific). Each of the peeper cells was sequentially removed from the solution at intervals depicted in Fig. 3 over one 24-h experiment, and the internal peeper cell concentrations of Br^- and Cl^- ions were measured via ion chromatography (AS-18 column, isocratic elution with KOH, DX-2000, Dionex Corporation). Figure 3 depicts the experimental measurement of Br^- and Cl^- concentration in the cells plotted as $\ln(C_p^t/C_p^i)$ versus time. The slope of this Br^- linear regression line is equivalent to the measured K_{Br} value for the experiment. In Fig. 3, K_{Br} estimated from only initial and final concentrations (two-point line) is used to calculate the expected Cl^- concentration in the

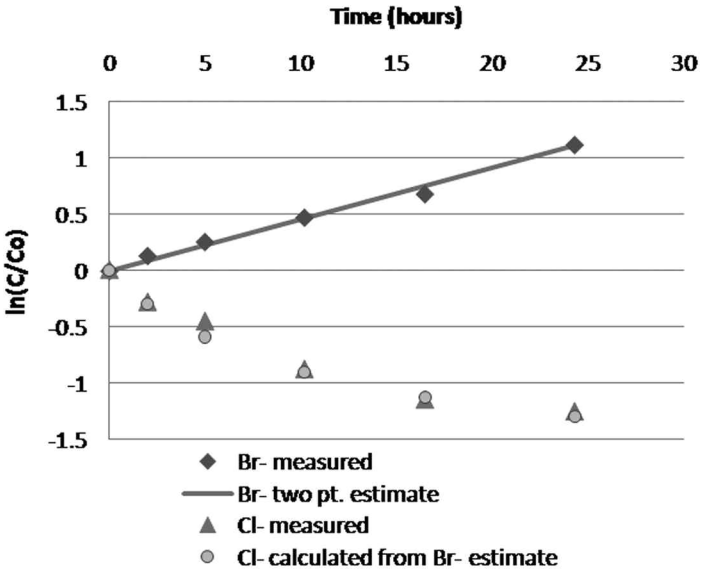

Fig. 3. Comparison of a time series of measured chloride concentrations, with the estimated chloride concentration in each cell given an initial and final measurement of chloride and bromide using Eq. 7.

beaker given a known initial chloride value in the peeper cell of 25 μM. The close agreement between measured and calculated (or corrected) Cl^- contents demonstrates that the chloride concentration determined from a two-point tracer–determined K value accurately estimates the measured inward-diffusing chloride ion content with time.

Equation 4 is appropriate for peeper cells in which the primary resistance to transport is diffusion across a membrane, likely the case within open water above the sediment–water interface. By adhering to the expression in Eq. 4, we are effectively assuming a shape of the time-dependent concentration curve that may not be accurate for peeper cells buried below the sediment–water interface, where the diffusion of ions to the membrane surface may be slow relative to transport across the membrane. In this common situation, the time-dependent concentration of a species in a peeper cell depends also on the rates of diffusion within the surrounding sediment and may not necessarily be described by the exponential decay expression in Eq. 4. For these situations, we can compare the exponential correction to other equations that approximate diffusion in solids. Ideally, we would be able to conduct experiments as above but in natural sediments. However, structural characteristics and inherent heterogeneity in natural sediments endangers the necessary assumption that samples would be replicates. Rather than resort to contrived homogenized sediment, we chose to perform model simulations to explore the behavior of the tracer in sediments.

Comparing analytical approximations—We adapted analytical approximations for diffusion from Carlslaw and Jaeger (1959) to compare the families of curves that represent diffusion from instantaneous point and plane sources. For the case of an infinite plane,

$$\Delta C_p = \Delta C_i(\pi kt)^{-1/2}, \tag{8}$$

and for the case of an infinite point,

$$\Delta C_p = \Delta C_i(\pi kt)^{-3/2}, \tag{9}$$

where $\Delta C_p = C^t_p - C^i_p$ and $\Delta C_i = C^i_{sed} - C^i_p$.

These expressions can be simplified to solve for the empirically derived constant, K_{Br}, given a one-point measurement of the outward diffusion of a tracer. This K_{Br} is analogous to that described in the case for diffusion across a cell membrane; however, in the case of diffusion in sediments, the physical meaning of this K value is obscured because it incorporates several potential sediment characteristics. By assuming the initial external tracer concentration is zero and the initial peeper solute concentration is zero, we can rearrange and simplify these three analytical expressions for the calculation of K_{Br} and for the initial concentration of solute in the sediment. For each of the three curve families, expressions are presented in Table 2.

As noted by Carlslaw and Jaeger (1959) the infinite plane and point source approximations are erroneous for small values of Kt. We can simplify this condition to state that the application of the point and plane peeper corrections requires a peeper tracer cell concentration of 40% or less of the starting value. The exponential decay curve family is not subject to this limitation, as it is an exact solution.

Model simulation—As a means to compare the effectiveness of these analytical expressions, we used a mathematical simulation of ion diffusion in sediments. We simulated this system with an explicit finite difference approximation for the spherically symmetric representation of Fick's second law (Carlslaw and Jaeger 1959):

$$\frac{\partial C}{\partial t} = D\left(\frac{\partial^2 C}{\partial r^2} + \frac{2}{r}\frac{\partial C}{\partial r}\right). \tag{10}$$

We coupled a discretization of the above expression for diffusion within sediment to an approximation of the Fick's first law–dependent flux across a peeper cell membrane. The peeper cell is treated as a sphere with a membrane area equivalent to the area of the sphere. Solute diffuses within the sediment according to Eq. 10. Separate permeation and diffusion parameters are applied for each solute. All model parameters were well within the strict stability and accuracy requirements of this discretization. We restricted our simulation to conservative solute behavior. The model presented here does not apply for solutes that participate in significant adsorption/desorption behavior, as is expected for trace metals and certain organic constituents (Harper et al. 1997), because an additional production/reaction term would be required. Given very rapid resupply via desorption or dissolution from a solid phase, we would expect behavior within sediments to approximate membrane permeation in solution as depicted in our bench-top experiments, because a lower concentration near-cell environment cannot develop.

For modeling purposes, all solutes started at 1 mM concen-

Table 2. List of analytical approximations for peeper correction calculations.

	Exponential Decay	Infinite plane source	Infinite point source
1	$\Delta C_p = \Delta C_i(1 - e^{-kt})$	$\Delta C_p = \Delta C_i(\pi kt)^{-1/2}$	$\Delta C_p = \Delta C_i(\pi kt)^{-3/2}$
2	$K_{Br} = -\frac{1}{t} ln\left(C^t_p / C^i_p\right)$	$K_{Br} = -\frac{1}{\pi t}\left(C^i_p / C^t_p\right)^2$	$K_{Br} = -\frac{1}{\pi t}\left(C^i_p / C^t_p\right)^{2/3}$
3	$C^i_{out} = C^t_p / (1 - e^{-K_i t})$	$C^i_{out} = C^t_p / (1 - (\pi K_i t)^{-1/2})$	$C^i_{out} = C^t_p / (1 - (\pi K_i t)^{-3/2})$

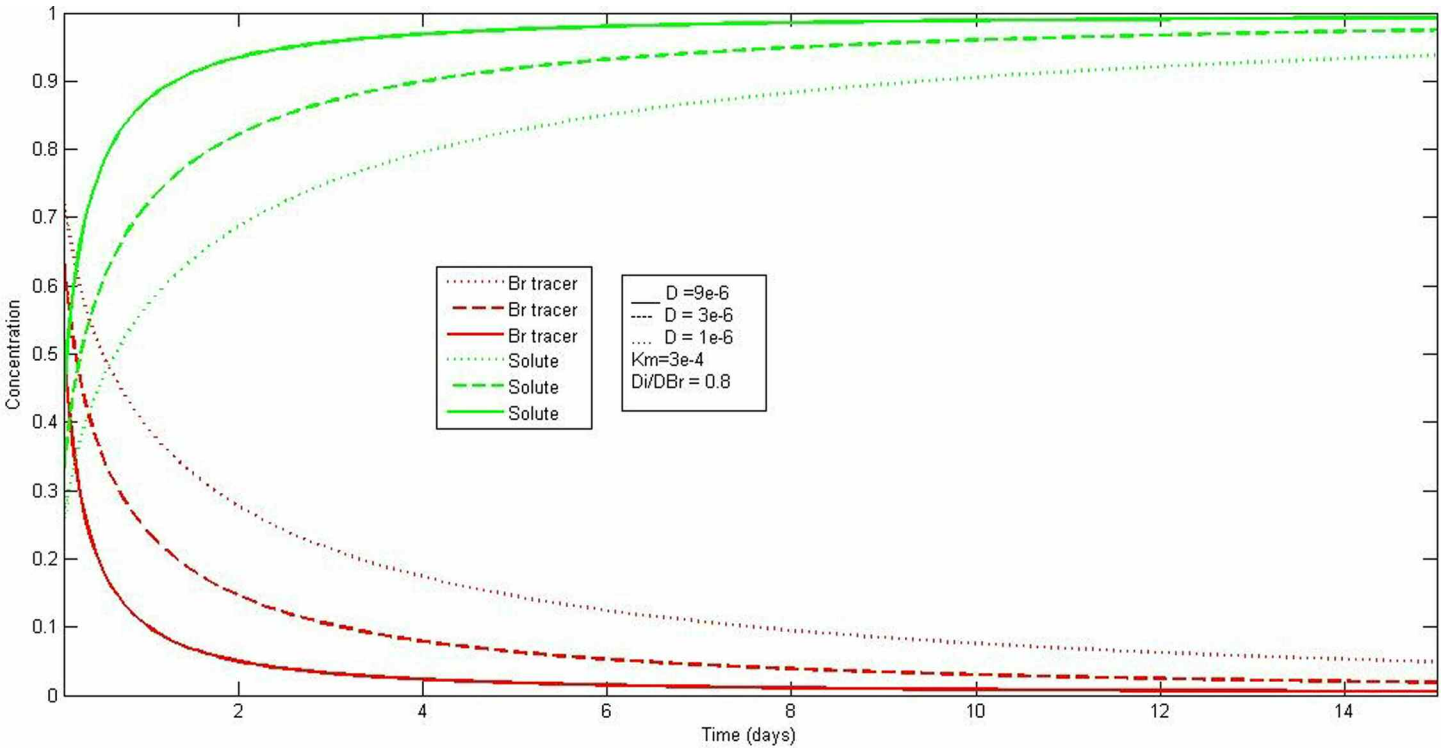

Fig. 4. Model results of the concentration of an outward-diffusing tracer and an inward-diffusing solute for each of three different sediment diffusivities, 1, 3, and 9 × 10^{-6} cm^2/s.

tration in sediments and all tracers started at 1 mM concentration in the cells. The simple model results of a 15-day simulation are plotted in Fig. 4 for a solute with D equivalent to 0.8 D_{Br} and sediment diffusivity with respect to bromide ranging over an approximate order of magnitude. After 4 days of peeper deployment, as much as 20% of the original bromide concentration may still be present in the peeper cell for the lowest diffusivity case. If a cell was extracted and the solute contents were measured after 4 days, the measurement would result in an approximate 20% underestimation of the formation solute concentration. The longer a peeper cell is deployed, the smaller these errors will be. Figure 4 is also instructive if we consider a case in which a single peeper is designed to sample at three different depths and each depth has a formation factor that is approximately 3 times greater than the one above. If each cell was sampled after 4 days, the topmost cell would be very near equilibrium, whereas the other cells might underestimate the formation content by as much as 10% to 20%.

Importance of species-specific K values—One frequently overlooked concern regarding peeper applications is that the solutes of interest might have diffusion constants that vary by a factor of 3 or more. So, in addition to being able to correct a single cell for incomplete equilibration, it may be important to apply a different correction for each solute if the diffusion constants are significantly different. Using our model, we can explore the importance of applying a species-specific correction to measured values. Figure 5 depicts the difference in cell concentration given outward diffusion of three different ions corresponding to sulfate, bromide, and hydroxide ion. We ran

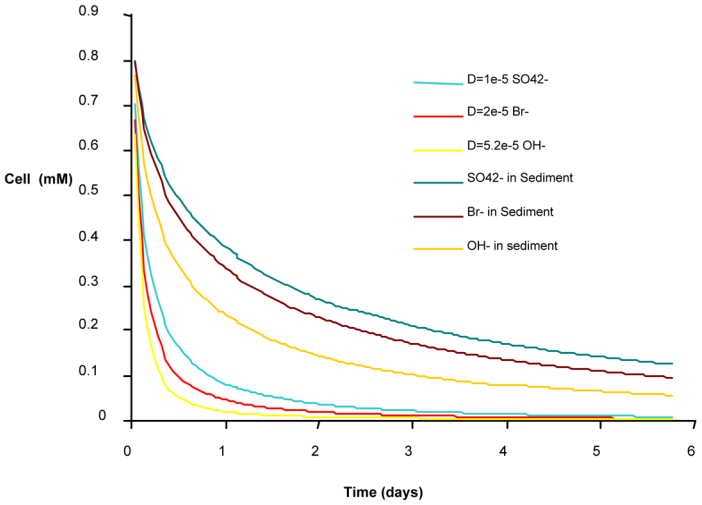

Fig. 5. Modeled time series within a peeper cell given outward diffusion of three different species beginning with an inward concentration of 1 mM. The two sets of curves represent cases in which diffusion is similar to diffusion in aqueous solution and one in which diffusion is hampered by sediment factors that decrease effective diffusivities by a factor of 10. This is roughly equivalent to the difference between open water and clay-rich sediment with 30% porosity.

two simulations of these ions given sediment conditions equivalent to open water and one equivalent to diffusion in clay-rich sediments.

As seen in Fig. 5, correcting peeper cell data requires both an estimation of the effective diffusivity of the sediment and an adjustment for the particular solute. The application of a reverse tracer accomplishes both. Using equations in the second row of Table 2, we can obtain a cell-specific empirical value for K_{Br}. Then, applying Eq. 6, we estimate a solute-specific K value to correct for each solute within each cell. The empirically derived K_{Br} incorporates any differences in temperature or tortuosity that affect sediment diffusivity. We do assume, however, that temperature and tortuosity are constants throughout the deployment time, a realistic assumption for most sediment systems.

Sensitivity to the choice of analytical expression—As a means to explore the sensitivity of our peeper corrections, we used the model output as synthetic data to predict the concentration of solute in the formation. We set the initial concentration of tracer inside the peeper and solute outside the peeper at 1 mM and provided different permeation speeds and diffusivities for the solutes. At each time step, we calculated the accuracy of an estimate of the formation solute concentration based solely on our modeled cell concentration of bromide, cell concentration of inward-diffusing solute, and time. These estimates produced concentration curves to compare to the "known" porewater concentration and to the uncorrected modeled cell concentration.

We performed a set of model simulations to compare each analytical expression for each of three different sediment diffusivities that correspond to an approximate 1 order of magnitude variation in D_e. Figure 6 depicts these results and shows that for diffusivities similar to open water (approaching 1*e*–5), the errors associated with uncorrected cell measurements

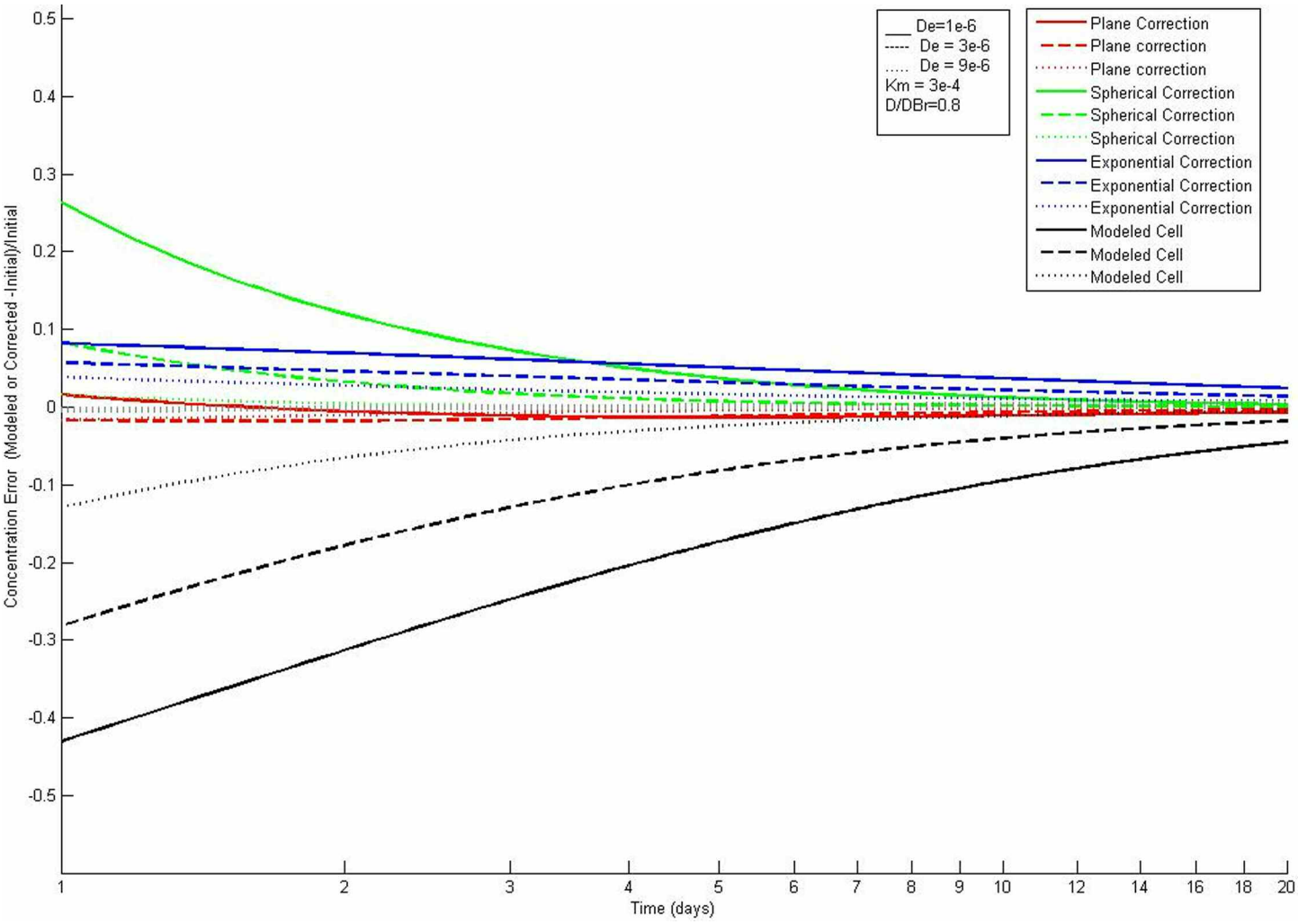

Fig. 6. For three bulk sediment diffusivities, we plotted the difference between the known external concentration and the modeled time series for four model cases. One represents uncorrected cell concentrations (black), and three represent the exponential, spherical, and plane corrections (blue, green, and red, respectively). Negative values are underestimates, positive values are overestimates. For low diffusivities, the exponential correction is everywhere superior to the uncorrected case.

would be on the order of 10% or less after 1 day. In consolidated or low diffusivity sediments, the outperformance of each correction increases dramatically and exists throughout the 3-week deployment. Clearly, the measured values would at all times underestimate the formation concentration, whereas the corrected values are typically only slight overestimates. Especially in consolidated sediment, even after 14 days, the modeled cell values would underestimate the actual concentration by approximately 10%, and each of the corrections would yield more accurate values than uncorrected values.

In Fig. 7, we compare the sensitivity of correction estimates to changes in the permeation speed of the peeper cell membrane. For each K_m value applied, the estimated errors are far better than the uncorrected values. Furthermore, the spherical correction appears to be most sensitive to lower-permeability peeper cell membranes, whereas the plane and exponential corrections are relatively less sensitive. The plane correction appears to outperform the others for all times; however, the spherical correction is accurate to 5% within the first week of deployment. Also, it is important to note that as the permeation speed of the membrane is decreased, the errors associated with uncorrected values increase.

We also tested the sensitivity of errors to different ion diffusion coefficients compared to bromide ion. Because compounds that diffuse faster than bromide will more quickly approach concentration equilibrium with the surrounding sediment, we expected that this method would be more useful for slowly diffusing compounds. The results of this sensitivity test are shown in Fig. 8. Bromide ion has a very high diffusivity compared to most other anions because it has a small solvation shell. As a result, most ions of interest will diffuse slower than bromide. As can be seen in Fig. 8, the accuracy of spherical and exponential estimates with a diffusivity ratio of 0.6 are on the whole not much better than the uncorrected estimate. The plane correction outperforms the others given low solute diffusivities.

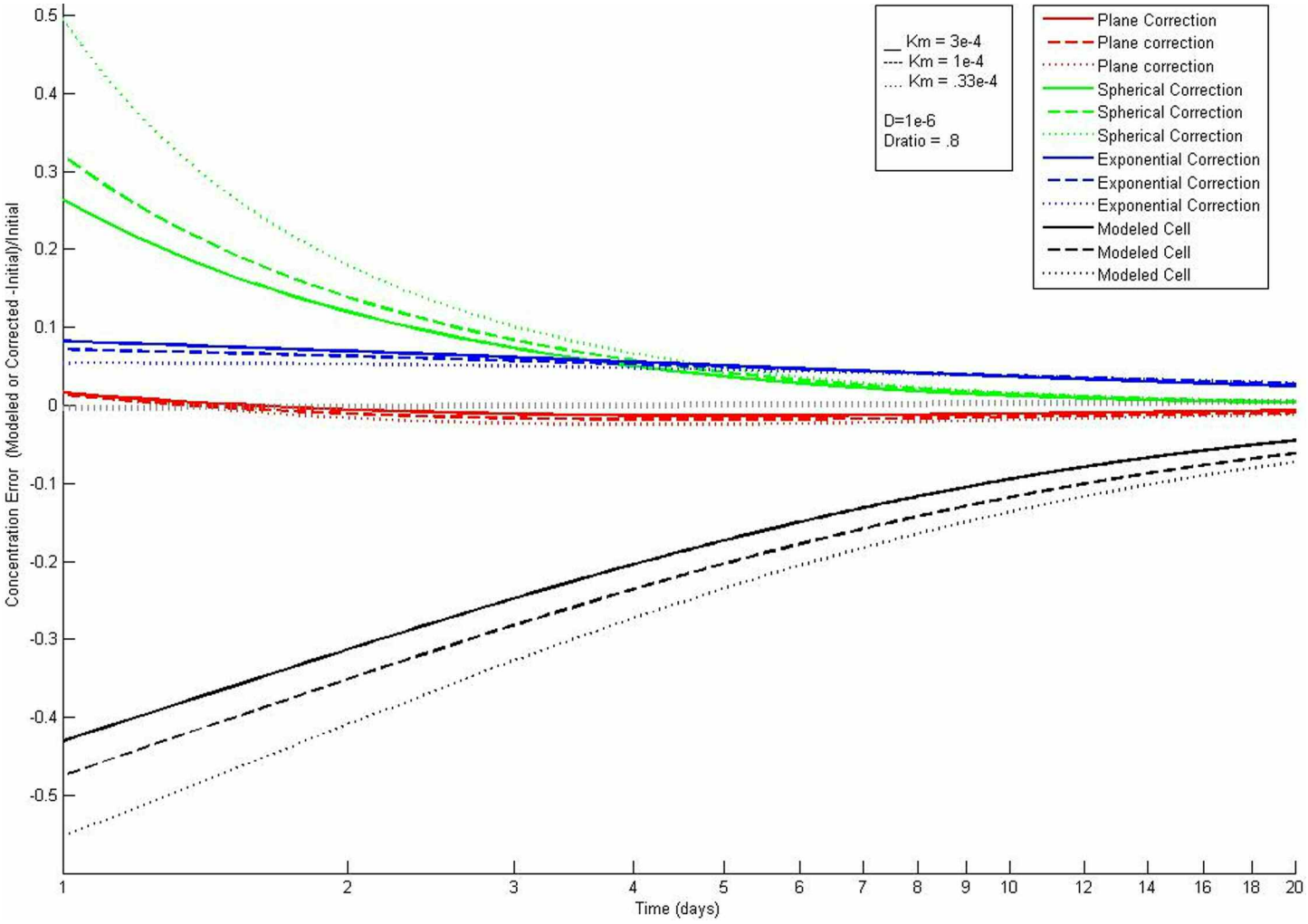

Fig. 7. Comparison of each analytical curve estimate with the uncorrected model cell concentrations. The *y*-axis represents the error in the estimate, and the *x*-axis is in log time.

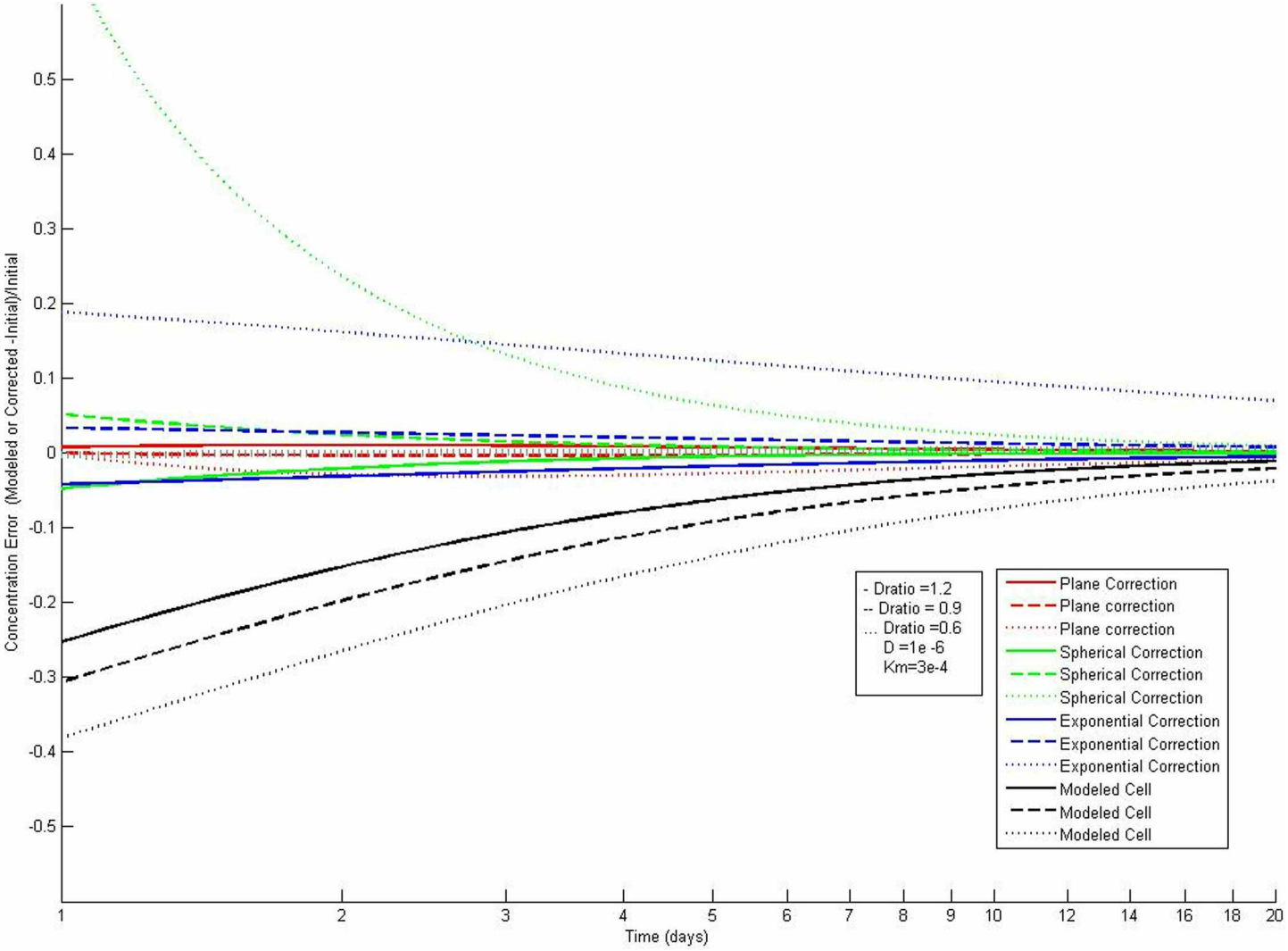

Fig. 8. Sensitivity of the corrected estimates to the diffusivity ratio of solute to bromide ion.

Discussion

As shown in the results of the field example application depicted in Fig. 2b–e, the measured concentrations of tracer remaining in the cells belie significant underestimates of formation solute concentrations. Each of the cell corrections results in small-magnitude positive adjustments in concentration; however, for the case of the solute with the lowest D_i/D_{Br} ratio, phosphate, the spherical correction is erroneous. This is also demonstrated in a sensitivity test to the diffusivity ratio depicted in Fig. 8. The analytical point source (spherical) equation is likely a poor choice for most sediment environments since its accuracy becomes superior only at very long deployment times where the need for correction is less severe.

The common assumption that a single length of deployment is sufficient to reach concentration equilibrium in all cells is rarely based on site-specific studies. Furthermore, site-specific assessments are incapable of accounting for local heterogeneity. In systems where it is impractical to apply a simple depth-dependent diffusivity, and for peeper deployments that may impact unknown local sediment characteristics, this reverse tracer technique can be used to estimate the extent of equilibrium and to correct measured concentrations for the effects of variable diffusivity.

Of the three families of curves we highlighted, the significant inaccuracy inherent in the spherical approximation at low values of *Kt* limits its usefulness, whereas the plane and exponential correction improve on uncorrected peeper measurements for all deployment lengths. In the interest of simplicity, we propose that a simple correction based on the exponential decay form of the concentration curve is sufficient to dramatically improve peeper estimates of sediment and soil porewater concentrations at all peeper deployment lengths.

References

Bender, M., W. Martin, J. Hess, F. Sayles, L. Ball, and C. A. Lambert. 1987. Whole-core squeezer for interfacial pore-water sampling. Limnol. Oceanogr. 32:1214-1225. [doi:10.4319/lo.1987.32.6.1214].

Blodau, C., and T. R. Moore. 2002. Macroporosity affects water movement and pore water sampling in peat soils. Soil Sci. 167:98-109. [doi:10.1097/00010694-200202000-00002].

Brandl, H., K. W. Hanselmann, R. Bachofen, and J. Piccard. 1993. Small-scale patchiness in the chemistry and microbiology of sediments in Lake Geneva, Switzerland. J. Gen. Microbiol. 139:2271-2275.

Carlslaw, H. S., and J. C. Jaeger. 1959. Conduction of heat in solids. Oxford Science Publications.

Dattagupta, S., G. Telesnicki, K. Luley, B. Predmore, M. McGinley, and C. R. Fisher. 2007. Submersible operated peepers for collecting porewater from deep-sea sediments. Limnol. Oceanogr. Methods 5:263-268.

Harper, P. M., W. Davison, and W. Tych. 1997. Temporal, spatial, and resolution constraints for in situ sampling devices using diffusional equilibration: Dialysis and DET. Environ. Sci. Technol. 31:3110–3119. [doi:10.1021/es9700515].

Hayduk, W., and H. Laudie. 1974. Prediction of diffusion-coefficients for nonelectrolytes in dilute aqueous-solutions. Aiche J. 20:611-615. [doi:10.1002/aic.690200329].

Hesslein, R. H. 1976. In situ sampler for close interval pore water studies. Limnol. Oceanogr. 21:912-914. [doi:10.4319/lo.1976.21.6.0912].

LaForce, M. J., C. M. Hansel, and S. Fendorf. 1999. Constructing simple wetland sampling devices. Soil Sci. Soc. Am. J. 64:809-811.

Lewandowski, J., K. Ruter, and M. Hupfer. 2002. Two-dimensional small-scale variability of pore water phosphate in freshwater lakes: Results from a novel dialysis sampler. Environ. Sci. Technol. 36:2039-2047. [doi:10.1021/es0102538].

Li, Y. H., and S. Gregory. 1974. Diffusion of ions in sea-water and in deep-sea sediments. Geochim. Cosmochim. Acta 38:703-714. [doi:10.1016/0016-7037(74)90145-8].

Lyons, W. B., H. E. Gaudette, and G. M. Smith. 1979. Pore water sampling in anoxic carbonate sediments: Oxidation artifacts. Nature 277:48-49.

Mayer, L. M. 1976. Chemical water sampling in lakes and sediments with dialysis bags. Limnol. Oceanogr. 21:909-912.

Reeburgh, W. S. 1967. An improved interstitial water sampler. Limnol. Oceanogr. 12:163. [doi:10.4319/lo.1967.12.1.0163].

Sayles, F. L., T. R. S. Wilson, D. N. Hume, and P. Mangelsd. 1973. In-situ sampler for marine sedimentary pore waters: Evidence for potassium depletion and calcium enrichment. Science 181:154-156.

Webster, I. T., P. R. Teasdale, and N. J. Grigg. 1998. Theoretical and experimental analysis of peeper equilibration dynamics. Environ. Sci. Technol. 32:1727-1733. [doi:10.1021/es970815g].

Submitted 28 December 2009
Revised 17 May 2010
Accepted 19 June 2010